Supporting Information

Russell et al. 10.1073/pnas.1006461108

SI Text

FTIR Measurements and Analysis Techniques. FTIR analysis was performed on Teflon filters downstream of a 1-μm impactor (SCC 2.229PM1, BGI Inc.). FTIR spectroscopy measures the absorption of organic functional groups associated with the frequency of a particular type of bond. These functional groups include "alkane groups" that consist of saturated aliphatic C-CH bonds (which are found in molecules such as alkanes as well as many other organic molecules, as they constitute hydrocarbon chains). The three most common oxygen-containing functional groups may include "carboxylic acid groups" (COH and C = O present on the same C atom, namely COOH and found in carboxylic acids and diacids), nonacid "carbonyl groups" (C = O without COH on the same C atom, as found in ketones, aldehydes, and esters, although the detectable peaks have to date ruled out aldehydes), and "hydroxyl groups" (COH without C = O on the same C atom, as found in straight chain alcohols, hydroxynitrates, polyols such as triols and tetrols, and saccharides such as sugars, cellulose, and starches). In addition, nitrogen- and sulfur-containing groups include "amine groups" (C-NH_2, as found in primary amines), "organosulfate groups" (C-OSO_3), and "organonitrate groups" (C-ONO_2). Aromatic and unsaturated aliphatic (or "alkene") groups were below detection for more than 80% of samples in each campaign and are omitted from this discussion, recognizing that these groups may account for as much as the detection limit of each sample, which ranged from 2 to 5% of organic mass (OM) depending on sample loading. Bond absorption is measured by transmission directly through the Teflon filter, with peak fitting and integration algorithms that minimize bias (1), and absorption is converted to mass by reference to calibration standards that have been shown to represent atmospheric organic composition with uncertainties of up to 20% for OM and 30% for individual functional groups (2–4). The mass for each functional group is defined to be the average mass associated with that group in typically observed atmospheric molecules; carboxylic acid and nonacid carbonyl groups are assumed to include one carbon atom and all heteroatoms in the group, but saturated aliphatic alkane groups and hydroxyl groups are approximated as nonterminal and include the mass of only half a carbon atom in addition to the heteroatoms. These approximations have been shown to result in OM measurements comparable to other techniques (3, 4).

The atmospheric measurement campaigns in which FTIR was used to quantify organic functional groups are summarized in Table 1. The four campaigns before 2004 were carried out using an FTIR facility at Rutgers University with a Mattson Research Series 100 FTIR Spectrometer with a deuterated triglycine sulfate (DTGS) detector in a temperature-controlled room as described by Maria et al. (3, 5, 6). FTIR measurements from the 17 campaigns between 2004 to 2009 were conducted using a Tensor 27 spectrometer with a DTGS detector (Bruker Optics) in a humidity- and temperature-controlled cleanroom, for which new calibration standards and an automated algorithm have been used to improve identification and precision of additional functional groups, including carboxylic acid, organic hydroxyl, and nonacid carbonyl groups (1). Each campaign dataset contains between 50–100 samples, each collected for typically between 6- and 24-h duration.

Each of the measured functional groups is calibrated with standards to obtain a detector-specific absorptivity relating the absorbance to the number of bonds, from which the mass of functional groups is estimated (2). The method uses typical organic carbon (OC) chain lengths in the atmosphere to associate a mass of carbon with each group (i.e., an average of two noncarbon bonds per carbon atom) and sums the resulting mass to determine OM (2). Comparisons of the resulting OM and OC measurements agreed within the accuracy of evolved gas analysis techniques (3–5). Comparisons of eight field projects with colocated aerosol mass spectrometry (AMS) measurements resulted in an overall slope of 0.99 and a correlation coefficient ($r = 0.80$), although individual projects ranged from reporting 30% less OM than AMS OM [corrected by collection efficiency (CE)] concentrations to more than a factor of 2 more than CE-corrected AMS OM concentrations in conditions with high mass modes of submicron solid particles (7, 8). Consequently, there is substantial evidence that bounds the OM not measured by FTIR to be less than 20%; this 20% may represent the mass of organic groups not detected or not calibrated by this technique (for which we choose not to apply a collection efficiency because of the lack of an independent basis on which to estimate the fraction missed).

Comparison of Field Campaigns and OM Source Attribution. In addition to our earlier reports of organosulfate groups during the International Consortium for Atmospheric Research on Transport and Transformation (ICARTT) and the Asian Pacific Regional Aerosol Characterization Experiment (ACE-Asia) (3, 4), organosulfates have been identified in the Southeastern United States and in Hungary (9, 10). However, the most frequent contribution of organosulfate groups was in the eastern North Atlantic and north of the Arctic Circle during April 2008, primarily from European-influenced air masses. The low ammonium concentrations coincident with these observations are consistent with laboratory results showing acid-catalyzed formation of organosulfates (11).

There is not yet clear evidence for organosulfates from biogenic sources in the regions we studied, as only a handful of samples from Whistler (British Columbia, Canada) and ICARTT showed absorption by organosulfate functional groups. In most of the conditions for which organosulfate groups were measured, OM exceeds 1 $\mu g\,m^{-3}$ and inorganic sulfate exceeds inorganic nitrate (4, 8, 12, 13). The high OM concentrations and high sulfate mass fractions were observed most frequently in regions of the International Chemistry Experiment in the Arctic LOwer Troposphere (ICEALOT) and the VAMOS Ocean-Cloud-Atmosphere-Land Study (VOCALS) that were dominated by combustion emissions with collocated emissions of both sulfate and OM precursors. In a similar and complementary way, organonitrate groups were only detected in the winter at Scripps Pier (La Jolla, California), when OM exceeded 1 $\mu g\,m^{-3}$ and submicron inorganic nitrate equaled or exceeded sulfate concentrations (14). In addition, there is indirect evidence suggesting that aqueous and acidic conditions favor particle phase reactions that produce organosulfates (8), and those same humid and acidic conditions may result in hydrolysis of organonitrate groups formed in the gas phase (14).

Applying a hierarchical clustering algorithm (15) sorts the samples into six categories based on similarities in absorption spectra that reflect mixtures of varying amounts of three types of contributions (urban, marine, forest), with the resulting average cluster compositions that are illustrated in Fig. S1. The clustering illustrates both strong similarities among Texas Air Quality Study (TexAQS), Megacity Initiative: Local and Global Research Operations (MILAGRO), and other urban sites for which com-

bustion sources are large, in addition to showing the shift in composition for the projects that are more dominated by marine influences in ICEALOT and Barrow (Alaska). This distribution of different types of organic aerosols in different regions is similar to that shown recently for a range of locations (16).

This type of algorithm presents a reasonable representation of typical ambient conditions and sources in the sampled regions, but a factorization rather than a clustering approach makes it possible to extract specific compositions associated with different sources in each region. Positive matrix factorization (PMF) (17) was implemented as our multivariate curve resolution technique to statistically reduce 1,368 ambient spectra from 12 of the campaigns into a few "components" that share significant covariation in absorbance across wavenumbers, as described by Russell et al. (1). For each project identified in Table 1, we systematically explored the solution space of two parameters: number of factors (p) and rotation parameter (FPEAK). We applied singular value decomposition to each dataset and also sectionally, by fixed-size moving window analysis (18). The trace of eigenvalues in each case was used to constrain the value of p to those values that provided sufficient data reconstruction (approximately 90% data recovery). As expected, the limited number of samples in the 30- to 120-d campaigns (100 to 150) allowed typically four factors to be identified that were either not correlated to each other or were indistinguishable from blanks. For each project, each factor was identified based on mild or strong correlations to elemental markers in the particle phase or to potential volatile organic compound aerosol-precursors in the gas phase. The details of these correlations for each campaign are described elsewhere (1, 12, 8, 14; 19–23).

Representative Reactions for Alkane Oxidation. The alkane, alkene, and cyclic alkene reactions discussed in the main text are illustrated by the schematic reactions in Fig. S2.

1. Russell LM, et al. (2009) Oxygenated fraction and mass of organic aerosol from direct emission and atmospheric processing measured on the R/V *Ronald Brown* during TEXAQS/GoMACCS 2006. *J Geophys Res* 114: D00F05, 10.1029/2008JD011275.
2. Russell LM (2003) Aerosol organic-mass-to-organic-carbon ratio measurements. *Environ Sci Technol* 37:2982–2987.
3. Maria SF, et al. (2003) Source signatures of carbon monoxide and organic functional groups in Asian Pacific Regional Aerosol Characterization Experiment (ACE-Asia) submicron aerosol types. *J Geophys Res* 108, 10.1029/2003JD003703.
4. Gilardoni S, et al. (2007) Regional variation of organic functional groups in aerosol particles on four U.S. east coast platforms during the International Consortium for Atmospheric Research on Transport and Transformation 2004 campaign. *J Geophys Res*, 112, 10.1029/2006JD007737.
5. Maria SF, et al. (2002) FTIR measurements of functional groups and organic mass in aerosol samples over the Caribbean. *Atmos Environ* 36:5185–5196.
6. Maria SF, Russell LM (2005) Organic and inorganic aerosol below-cloud scavenging by suburban New Jersey precipitation. *Atmos Environ* 39:4793–4800.
7. Russell LM, et al. (2003) Organic aerosol characterization by complementary measurements of chemical bonds and molecular fragments. *Atmos Environ* 43:6100–6105, 10.1016/j.atmosenv.2009.09.036.
8. Hawkins LN, et al. (2010) Carboxylic acids, sulfates, and organosulfates in processed continental organic aerosol over the Southeast Pacific Ocean during VOCALS-REx 2008. *J Geophys Res* 115:D13201, 10.1029/2009JD013276.
9. Surratt JD, et al. (2007) Effect of acidity on secondary organic aerosol formation from isoprene. *Environ Sci Technol* 41:5363–5369.
10. Gomez-Gonzalez Y, et al. (2008) Characterization of organosulfates from the photooxidation of isoprene and unsaturated fatty acids in ambient aerosol using liquid chromatography/(-) electrospray ionization mass spectrometry. *J Mass Spectrom* 43:371–382.
11. Surratt JD, et al. (2008) Organosulfate formation in biogenic secondary organic aerosol. *J Phys Chem A*, 112:8345–8378, 10.1021/jp802310p.
12. Russell LM, et al. (2010) Carbohydrate-like composition of submicron atmospheric particles and their production from ocean bubble bursting. *Proc Natl Acad Sci USA* 107:6652–6657.
13. Schwartz RE, et al. (2010) Biogenic oxidized organic functional groups from a mid-mountain forest at Whistler, BC, and their similarities to laboratory chamber products. *Atmos Chem Phys* 10: 5075–5088, 10.5194/acp-10-5075-2010.
14. Day DA, et al. (2010) Organonitrate group concentrations in submicron particles with high nitrate and organic fractions in coastal southern California. *Atmos Environ* 44:1970–1979.
15. Ward JH (1963) Hierarchical grouping to optimize an objective function, *J Am Stat Assoc* 58:236–244, 10.2307/2282967.
16. Jimenez JL, et al. (2009) Evolution of organic aerosols in the atmosphere. *Science* 326:1525–1529.
17. Paatero P, Tapper U (1994) Positive matrix factorization—A nonegative factor model with optimal utilization of error estimates of data values. *Environmetrics* 5:111–126.
18. Keller HR, Massart DL (1991) Evolving factor analysis. *Chemometr Intell Lab* 12:209–224.
19. Liu S, et al. (2009) Oxygenated organic functional groups and their sources in single and submicron organic particles in MILAGRO 2006 campaign. *Atmos Chem Phys* 9:6849–6863.
20. Bahadur R, et al. (2010) Phenol groups in Northeastern U.S. submicron aerosol particles produced from seawater sources. *Environ Sci Technol* 44:2542–2548, 10.1021/es9032277.
21. Day DA, et al. (2009) Organic composition of single and submicron particles in different regions of Western North America and the Eastern Pacific during INTEX-B 2006. *Atmos Chem Phys* 9:5433–5446.
22. Hawkins LN, Russell LM (2010) Oxidation of ketone groups in transported biomass burning aerosol from the 2008 Northern California Lightning Series fires. *Atmos Environ* 44:4142–4154, 10.1016/j.atmosenv.2010.07.036.
23. Shaw PM, et al. (2010) Arctic organic aerosol measurements show seasonal particle sources of spring haze and winter frost flowers. *Geophys Res Lett* 37:L10803, 10.1029/2010GL042831.

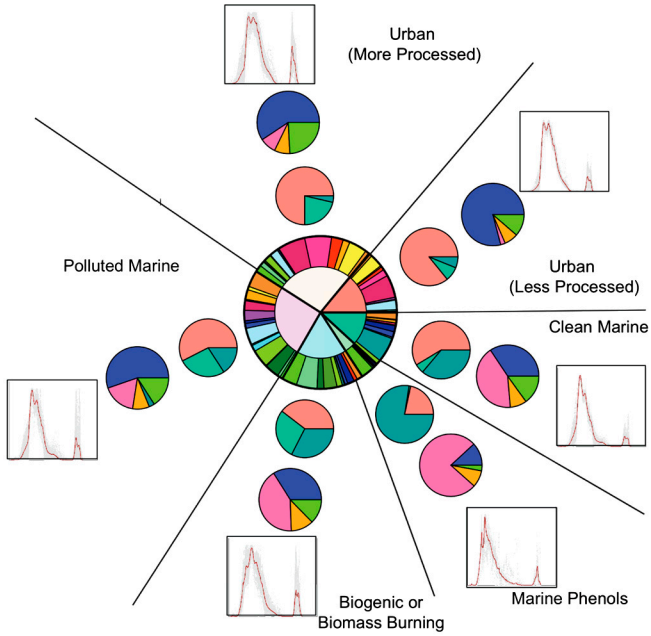

Fig. S1. Categories of submicron particle composition identified by Ward hierarchical clustering of 793 FTIR spectra. Colors in the central "pinwheel" pie chart indicate the number of 4- to 24-h samples from each of 17 measurement campaigns identified with each of six clusters, using the color scheme indicated by the arrows in Fig. 1. Colors in the pie charts outside the pinwheel for each category show factors obtained from PMF of FTIR spectra for each of the six clusters, with combustion in salmon, biogenic or biomass burning in jade, and marine or background in cerulean. Colors in the outermost pie charts indicate mass fraction of each group, showing alkane (blue), alcohol, including polyol (pink), amine (orange), nonacid carbonyl (teal), carboxylic acid (green), and organosulfate (yellow) group contributions. The outer graph shows the normalized absorbance by FTIR versus wavelength for the range of 1400 to 3600 cm^{-1} for all of the spectra in each cluster (in gray) and the cluster average (in red).

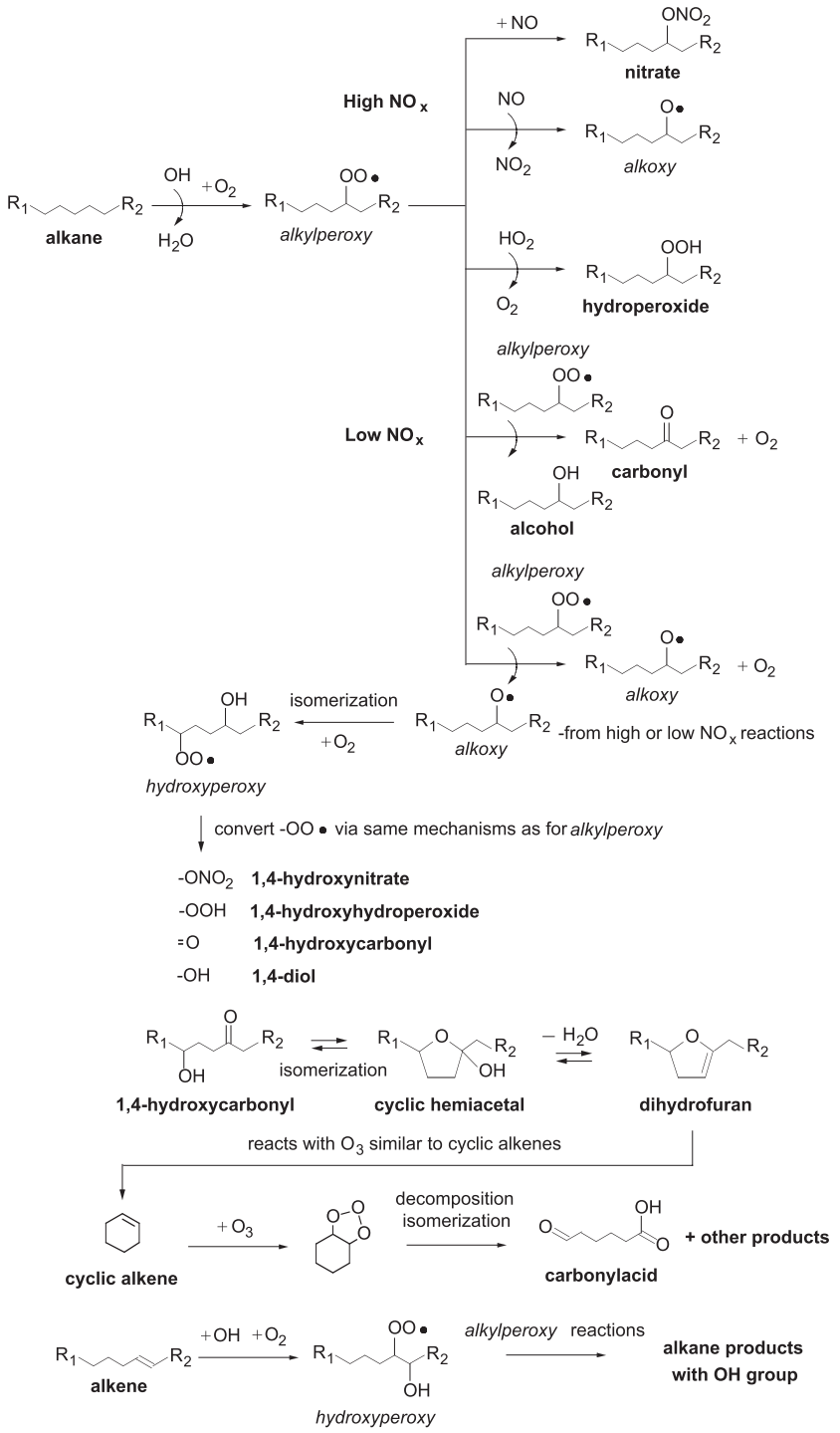

Fig. S2. Mechanism of OH radical-initiated reactions of alkanes and alkenes under high and low NO_x conditions to form first-generation monofunctional and multifunctional products, formation of dihydrofurans from 1,4-hydroxycarbonyls, and reaction of cyclic alkenes with O_3 to form carbonylacids. Other cyclic alkene reaction products contain similar functional groups to those formed from alkanes and alkenes, but also include carboxylic acids. Bold labels correspond to stable products, and italicized labels correspond to radical intermediates.